JOURNAL OF NEUROTRAUMA 29:201–217 (January 20, 2012)

DOI: 10.1089/neu.2011.1761

Traumatic Brain Injury Causes an FK506-Sensitive Loss and an Overgrowth of Dendritic Spines in Rat Forebrain

John N. Campbell,[1] David Register,[2] and Severn B. Churn[1–3]

Abstract

Traumatic brain injury (TBI) causes both an acute loss of tissue and a progressive injury through reactive processes such as excitotoxicity and inflammation. These processes may worsen neural dysfunction by altering neuronal circuitry beyond the focally-damaged tissue. One means of circuit alteration may involve dendritic spines, micron-sized protuberances of dendritic membrane that support most of the excitatory synapses in the brain. This study used a modified Golgi-Cox technique to track changes in spine density on the proximal dendrites of principal cells in rat forebrain regions. Spine density was assessed at 1 h, 24 h, and 1 week after a lateral fluid percussion TBI of moderate severity. At 1 h after TBI, no changes in spine density were observed in any of the brain regions examined. By 24 h after TBI, however, spine density had decreased in ipsilateral neocortex in layer II and III and dorsal dentate gyrus (dDG). This apparent loss of spines was prevented by a single, post-injury administration of the calcineurin inhibitor FK506. These results, together with those of a companion study, indicate an FK506-sensitive mechanism of dendritic spine loss in the TBI model. Furthermore, by 1 week after TBI, spine density had increased substantially above control levels, bilaterally in CA1 and CA3 and ipsilaterally in dDG. The apparent overgrowth of spines in CA1 is of particular interest, as it may explain previous reports of abnormal and potentially epileptogenic activity in this brain region.

Key words: calcineurin; cofilin; epilepsy; epileptogenesis; traumatic brain injury

Introduction

Survivors of traumatic brain injury (TBI), most of whom are young adults, often suffer lifelong disabilities. The devastating consequences of TBI derive in part from its progressive nature: the immediate, mechanical destruction of tissue can be followed by days to weeks of excitotoxic and inflammatory damage (Zipfel et al., 2000; Lenzlinger et al., 2001). This cumulative injury can alter neural function well beyond the focally-damaged tissue and so may contribute to TBI-induced neuropathologies, such as cognitive impairment and post-traumatic epilepsy. Animal modeling of TBI has revealed that cognitive impairment can occur in the absence of cell death (Lyeth et al., 1990), and that the onset of post-traumatic epilepsy (PTE) can be many months after TBI (Pitkanen and McIntosh, 2006). It is therefore likely that cognitive impairment and PTE develop from disruptions in neural circuitry beyond the acute loss of cells. A better understanding of how TBI disrupts neural circuitry should uncover novel therapeutic targets for treating TBI-induced neuropathologies.

One potential mechanism of disrupted neural circuitry may be the loss of dendritic spines. Dendritic spines are specialized protuberances of dendritic membrane which form the post-synaptic component of most excitatory synapses in the brain (Nimchinsky et al., 2002). The stability of the dendritic spine depends on synaptic activity (McKinney et al., 1999). Indeed, the loss of its pre-synaptic partner can cause the spine to retract into the dendritic shaft (Parnavelas et al., 1974), and spine collapse due to de-afferentation is a well-characterized phenomenon. However, an excess of synaptic activity can also cause spine collapse, through the toxic excitation of glutamate receptors (Park et al., 1996). Multiple post-synaptic mechanisms linking excitotoxicity to dendritic spine loss have been proposed and demonstrated *in vitro* (reviewed in Campbell et al., 2009). Interestingly, at least two of these mechanisms are mediated by the calcium-sensitive phosphatase, calcineurin (CaN) (Halpain et al., 1998; Pak and Sheng, 2003). Since CaN is activated by glutamate signaling (Halpain et al., 1990), and glutamate signaling occurs in excess after TBI (Choi, 1992), it is plausible that an increase in CaN activity leads to dendritic spine loss after TBI.

Departments of [1]Anatomy & Neurobiology, [2]Neurology, and [3]Pharmacology & Toxicology, Virginia Commonwealth University, Richmond, Virginia.

Here we report an extensive analysis of dendritic spine density in the laterally-injured brain. In addition, this study and its companion (Campbell et al., 2011) present evidence of CaN-dependent mechanisms by which TBI results in dendritic spine loss. In particular, this study describes a region-specific loss of dendritic spines which can be blocked by a single, post-injury injection of FK506, a pharmacological inhibitor of CaN. This spine loss coincides, temporally and regionally, with changes in cofilin activity observed in our companion study (Campbell et al., 2011). In addition, the spine loss is followed by an apparent overgrowth of dendritic spines in both hemispheres of the hippocampus. Overall, these findings suggest that the rat forebrain undergoes an extensive turnover of dendritic spines during recovery from lateral brain injury, which may participate in the development of cognitive impairment and post-traumatic epilepsy. Furthermore, these findings identify CaN as a potential therapeutic target in the treatment of TBI.

Methods

Use of animal subjects was performed in strict accordance with the *Guide for the Care and Use of Laboratory Animals*, provided by the National Institutes of Health (NIH), and approved in advance by the Virginia Commonwealth University Institutional Animal Care and Use Committee. Animal subjects received *ad libitum* access to food and water and were maintained on 12-h light/dark cycles throughout the experiment.

Surgical preparation and fluid percussion injury

Adult male Sprague-Dawley rats (90 days old; 350–400 g; $n = 21$) were anesthetized with sodium pentobarbital (54 mg/kg IP) and placed into a stereotactic frame. A 4.8-mm hole was made over the left hemisphere using a trephine centered 4 mm caudal to the bregma and −3 mm lateral to the sagittal suture. A screw was inserted over the opposite hemisphere to anchor the skull attachments. A modified female Luer-Loc syringe hub (2.6 mm inside diameter) was placed over the exposed dura, affixed with cyanoacrylate adhesive, and then secured with dental acrylic. On the following day, the subjects were anesthetized (4% isoflurane in a carrier gas mixture of 26% N_2O and 70% O_2) in a chamber, then removed from the chamber and immediately subjected to fluid percussion of the intact dura over the left parietal cortex. The fluid percussion device used in these experiments is identical to that described by Dixon and colleagues (Dixon et al., 1987). The Luer-Loc fitting, screw, and dental cement were removed from the skull immediately following injury. The subjects were then placed in a supine position and the time at which they righted themselves was recorded. Upon recovery of righting reflexes, the subjects were placed on a heating pad for at least 30 min (and up to 1 h) until ambulatory, then were returned to their home cages and monitored daily. At 1 h post-injury, some subjects received a single IP injection of FK506 (5 mg/kg; Fujisawa Chemical Company, Osaka, Japan).

Golgi-Cox histology and light microscopy

At 1 h, 24 h, and 1 week after lateral fluid percussion injury, the subjects were injected with a lethal dose of pentobarbital, perfused intracardially with saline (0.9%, 120 mL, room temperature), and decapitated. Brains were quickly extracted and immersed in a Golgi-Cox staining solution prepared from a commercially-available kit (FD Rapid Golgistain Kit; FD Neurotechnologies, Inc., Baltimore, MD). After 24 h of staining, the brains were blocked to remove tissue rostral and caudal to the hippocampus, immersed in fresh staining solution, and stored at room temperature in the dark for a total of 2 weeks. The remainder of the staining procedure was performed according to the kit instructions.

Following the staining procedure, the brains were cut into 200-μm-thick coronal sections using a vibratome (Leica, Wetzler, Germany). The sections were mounted onto 2% gelatin-coated slides and air-dried at room temperature in the dark overnight. Slide-mounted sections were developed and dehydrated according to the kit instructions, and cover-slipped with Permount.

Three brain sections nearest the injury site were selected for further analysis. Golgi-impregnated principal cells from the following regions were assessed for dendritic spine density: layers II and III of parietal neocortex penumbral to the site of injury ("ipsilateral neocortex$_{II,III}$"), and an analogous area of the contralateral hemisphere ("contralateral neocortex$_{II,III}$"); the pyramidal cell layer of the hippocampal subfields CA1 and CA3 in each hemisphere; and the granule cell layer of the dorsal leaf of the dentate gyrus (dDG; Fig. 1) in each hemisphere. Brain region identification was aided by a standard atlas of the rat brain (Paxinos and Watson, 1998). Golgi-stained principal cells were then visualized by light microscopy (Nikon Optiphot-2; Nikon Optiphot, Melville, NY). Under a 40× objective lens, pyramidal and granule neurons were identified by their location within cell layers and by the shape of their soma and dendritic arbor. Dendrites were visualized using a 100×/oil-immersion lens for manual tracing and dendritic spine quantification.

Dendrite tracing and dendritic spine quantification

To ensure consistency of sampling, the following inclusion criteria were applied. The dendrite sampled had to be (1) a second- or third-order branch, (2) within 30 μm–150 μm of the parent cell soma (as measured along the dendrite; "proximal"), (3) not obscured by other Golgi-stained tissue, (4) showing no signs of degeneration that would interfere with spine quantification (i.e., blebbing or beading of the proximal dendrite), and (5) connected to a soma that did not appear swollen or necrotic.

For each group of animals, at least 10 neurons per brain region per hemisphere were included in the analysis (for n values, see Supplementary Table 1; see online supplementary material at http://www.liebertonline.com). Fully-stained principal neurons within each region of interest were first selected under minimal magnification (4x objective). Under high magnification (100× oil-immersion objective), selected neurons were then screened according to the inclusion criteria described above. For each neuron, one proximal branch of dendrite was traced to a minimum length of 20 μm. With regard to granule cells of the dDG, only dendrites oriented dorsolaterally were analyzed. Dendrites were traced through the x-, y-, and z-planes using a digitizing microscope stage under control of Neurolucida (MicroBrightField, Inc., Williston, VT). The lengths of tracings were computed by Neurolucida Explorer software (MicroBrightField). Along each

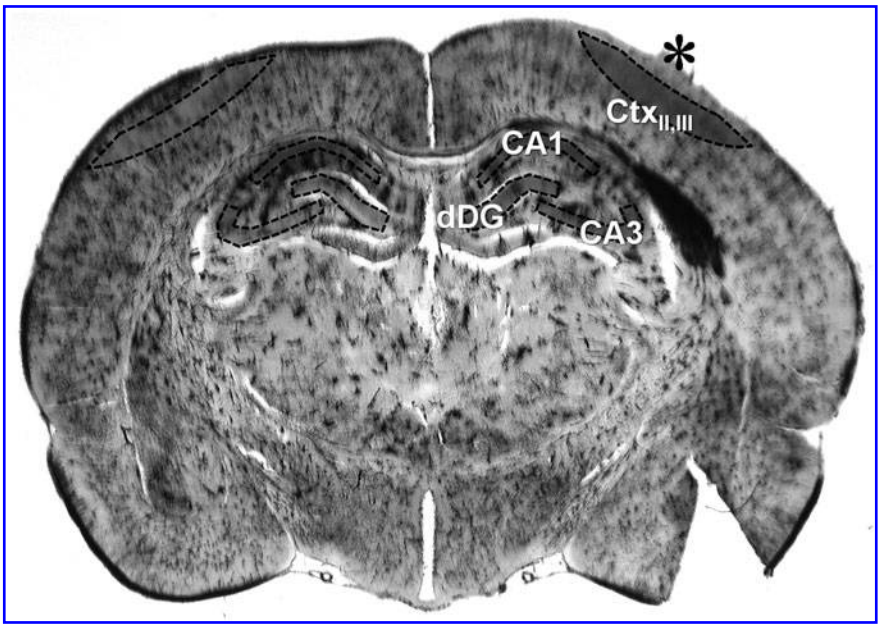

FIG. 1. Forebrain regions sampled for dendritic spine density. Shown is a micrograph of a Golgi-stained section of adult rat brain recovered 24 h after lateral fluid percussion injury of the left hemisphere. The approximate site of fluid percussion is indicated with an asterisk (*). Dendritic spine density was sampled in the shaded brain regions located ipsilateral and contralateral to the impact site, including layer II,III of the parietal neocortex (Ctx), the hippocampal subfields CA1 and CA3, and the dorsal leaf of the dentate gyrus (dDG). Analogous regions of uninjured brains were similarly assessed for spine density. Also visible in this image is where a wedge-shaped portion of ventral neocortex was excised prior to sectioning, to mark the ipsilateral hemisphere.

traced segment of dendrite, dendritic spines were counted according to their morphology (Fiala et al., 2008; Jones and Powell, 1969): thin spines and mushroom-shaped spines were counted together as "pedunculated spines," whereas spines lacking a neck constriction (e.g., stubby spines and filopodia-like spines) were counted as "non-pedunculated spines" (Fig. 2). Spine density was calculated as the number of spines visible along a traced segment of dendrite, divided by the length of the traced segment. No correction was made for spines not seen due to the angle or plane of section.

Statistical analyses

Mean spine densities in injured brains were statistically compared to those from the corresponding dendritic arbor and brain region of age- and drug treatment-matched control brains. Each mean was derived from a pool of spine densities obtained from 3 identically-treated rats. Student's *t*-tests were used to compare the FK506-treated injured group to the FK506-treated uninjured group, while one-way analysis of variance (ANOVA) with Tukey's *post-hoc* test was used for all other comparisons. Statistical analyses were performed with GraphPad Prism, version 5.0 (GraphPad Software, Inc., La Jolla, CA). Comparisons generating p values less than 0.05 were considered statistically significant. Data are presented as group mean ± standard error of the mean (SEM).

Results

Lateral fluid percussion injury

Adult male rats received a traumatic brain injury by fluid percussion of the dura overlying the left parietal cortex (mean pressure 2.22 ± 0.02 atm; between groups, $p > 0.05$). A common correlate of injury severity is the length of time between injury and the recovery of righting reflexes ("righting time"; Thompson et al., 2005). In the present study, the mean righting time was 8 min 52 sec ± 1 min 31 sec ($n = 12$), and was not significantly different between groups ($p > 0.05$). Some subjects exhibited apnea immediately following injury (5 out of 12 subjects) and were mechanically ventilated as needed (mean duration of ventilation, 1 min 32 sec ± 52 sec). All subjects survived the injury.

Dendritic spine quantification in injured and uninjured forebrain

To determine the effect of TBI on dendritic structure, brains were recovered 1 h, 24 h, and 1 week after lateral fluid percussion injury (LFPI) and subjected to a modified Golgi-Cox procedure (see methods section). Proximal dendrites (within 30–150 μm of soma) of Golgi-stained principal cells were manually traced (mean length of tracing ± standard deviation, 33.90 ± 9.43 μm) and spine density was quantified, in the following forebrain regions: neocortex$_{II,III}$ penumbral to the LFPI site ("ipsilateral neocortex$_{II,III}$") and in an analogous region of the contralateral hemisphere ("contralateral neocortex$_{II,III}$"); the hippocampal subfields CA1 and CA3; and the dorsal leaf of the dentate gyrus (dDG; Fig. 1). Mean densities of pedunculated spines (thin spines and mushroom-shaped spines; Fig. 2) and non-pedunculated spines (stubby spines and filopodia-like spines; Fig. 2) are provided in a supplementary table (Supplementary Table 1; see online supplementary material at http://www.liebertonline.com). Overall, 1,264 dendrites were traced and 57,372 dendritic spines were counted.

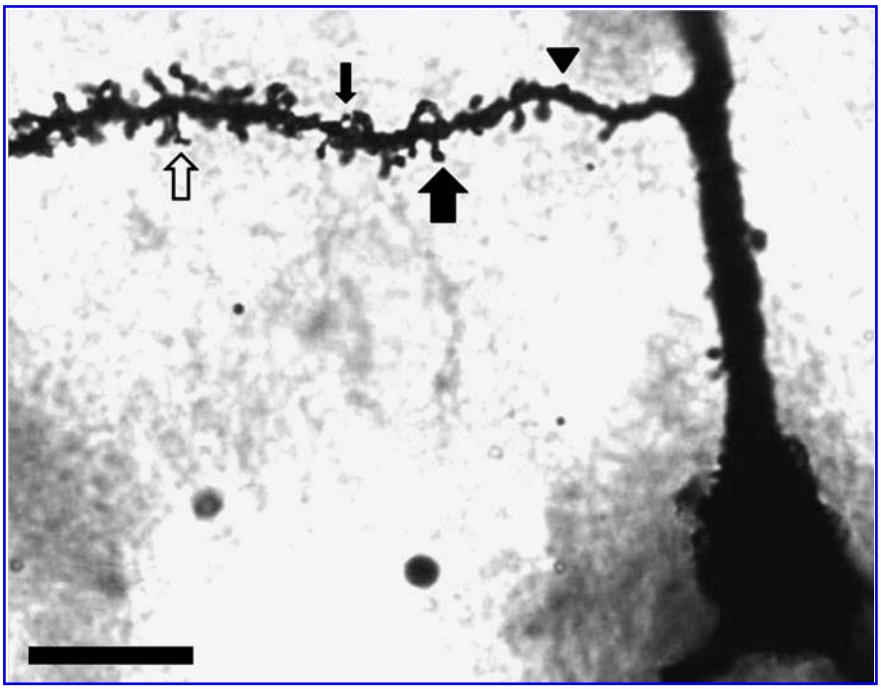

FIG. 2. Dendritic spines on a Golgi-stained pyramidal neuron from layer II,III of rat neocortex. A thin spine and a mushroom-shaped spine are marked, respectively, with a thin arrow and a thick arrow. A stubby spine and a filopodia-like spine are marked, respectively, with an arrowhead and a hollow arrow. Thin spines and mushroom-shaped spines were counted together as "pedunculated" spines, whereas stubby spines and filopodia-like spines were counted together as "non-pedunculated" spines. The arrowhead also approximates the minimum distance (30 μm) from the cell soma beyond which dendrites were traced and spine density was sampled (scale bar = 10 μm).

On apical dendrites in neocortex$_{II,III}$, lateral fluid percussion injury caused a transient decrease in spine density

Pyramidal cells in neocortex$_{II,III}$ receive excitatory synapses on spines throughout their apical and basilar dendritic arbors. To investigate the effect of traumatic brain injury on these dendritic spines, we began by assessing spine density on the apical dendrites of neocortex$_{II,III}$ pyramidal cells in control and laterally-injured brains (Fig. 3). In control brains, neocortex$_{II,III}$ pyramidal cells ($n = 14$) displayed an average of 1.20 ± 0.08 spines/μm on proximal apical dendrites, consistent with previously published data (Monfils and Teskey, 2004). This spine density included an average of 0.74 ± 0.05 pedunculated spines/μm, and an average of 0.46 ± 0.04 non-pedunculated spines/μm. At 1 h post-LFPI, the total spine density of these dendrites did not differ significantly from that of controls, in ipsilateral or contralateral neocortex$_{II,III}$ (each versus control, $p > 0.05$; Fig. 4A). Nor was the pedunculated or non-pedunculated spine density of these dendrites appreciably different from control values, in ipsilateral or contralateral neocortex$_{II,III}$ (each versus control, $p > 0.05$; Fig. 4B and C).

By 24 h post-LFPI however, apical dendrites in neocortex$_{II,III}$ showed a significant loss of spine density. Specifically, in ipsilateral neocortex$_{II,III}$, the total spine density of these dendrites decreased by 21% relative to controls ($p < 0.05$ versus control; Fig. 4A). Further analysis revealed an underlying change in the density of pedunculated spines: pedunculated spine density decreased 30% from control values ($p < 0.01$ versus control; Fig. 4B). Since the non-pedunculated spine density of these dendrites was relatively unchanged at this time ($p > 0.05$ versus control; Fig. 4C), it is likely that the loss of pedunculated spine density involved more than just a change in spine phenotype (i.e., from pedunculated to non-pedunculated). Furthermore, the effect on spine density appeared to be greater in the ipsilateral hemisphere. In contralateral neocortex$_{II,III}$, the pedunculated spine density of apical dendrites decreased 14% relative to controls, a change which was not statistically significant ($p > 0.05$ versus control; Fig. 4B). Thus, the data indicate that by 24 h post-LFPI there is a selective loss of pedunculated spine density from apical dendrites in ipsilateral neocortex$_{II,III}$. Because pedunculated spines are associated with stable synapses (Bourne and Harris, 2007), a decrease in their density could indicate synaptic re-modeling in the injured brain.

The decrease in pedunculated spine density was not permanent. By 1 week post-LFPI in ipsilateral neocortex$_{II,III}$, the pedunculated spine density of apical dendrites recovered to control levels ($p > 0.05$ versus control; Fig. 4B). Likewise in contralateral neocortex$_{II,III}$, the pedunculated spine density of these dendrites did not differ significantly from control values ($p > 0.05$ versus control; Fig. 4B). Nor was the non-pedunculated spine density altered relative to controls, in either hemisphere of neocortex$_{II,III}$ ($p > 0.05$ versus control; Fig. 4C). The data therefore describe a recovery in the pedunculated spine density of apical dendrites in neocortex$_{II,III}$ by 1 week post-LFPI.

Overall, these results suggest that lateral TBI transiently decreased the pedunculated spine density of apical dendrites in ipsilateral neocortex$_{II,III}$. This decrease is not likely due to acute mechanical trauma, as it occurred by 24 h but not by 1 h post-LFPI. The timing is more consistent with a secondary

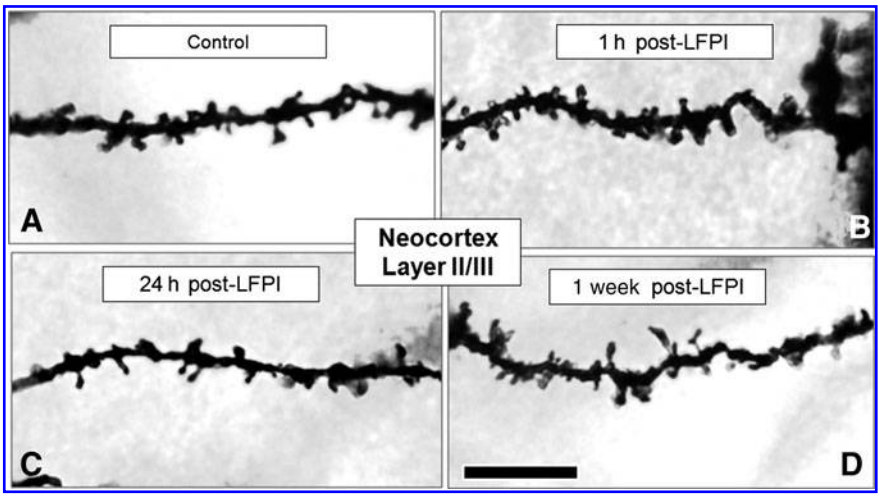

FIG. 3. Representative apical dendrites from Golgi-stained pyramidal cells in layer II,III neocortex. Shown are proximal dendrites (within 30–150 μm of cell soma) from the apical arbors of Golgi-stained pyramidal cells in rat neocortex layer II,III. Panel **A** shows a control dendrite with 8.10 pedunculated spines/10 μm (110% of group mean), and 4.05 non-pedunculated spines/10 μm (88% of group mean). Panels **B**, **C**, and **D** show dendrites in the penumbral region of the focal injury. Panel **B** shows a dendrite at 1 h post-LFPI, with 7.09 pedunculated spines/10 μm (102% of group mean), and 4.46 non-pedunculated spines/10 μm (92% of group mean). Panel **C** shows a dendrite at 24 h post-LFPI, with 4.89 pedunculated spines/10 μm (95% of group mean), and 4.14 non-pedunculated spines/10 μm (98% of group mean). Panel **D** shows a dendrite at 1 week post-LFPI, with 8.05 pedunculated spines/10 μm (119% of group mean), and 4.98 non-pedunculated spines/10 μm (117% of group mean). Note that not all spines counted are in focus in these micrographs (scale bar = 10 μm; LFPI, lateral fluid percussion injury).

injury process, such as excitotoxicity. Importantly, these changes in post-synaptic structure could indicate extensive alterations of neocortex$_{II,III}$ circuitry in the injured brain.

On basilar dendrites in neocortex$_{II,III}$, spine density fluctuated during recovery from lateral fluid percussion injury

Basilar dendrites in neocortex$_{II,III}$ were also studied in control and laterally-injured brains. In control brains, the proximal basilar dendrites of neocortex$_{II,III}$ pyramidals ($n = 13$) displayed 1.07 ± 0.04 spines/μm; a similar value has been reported previously (Monfils and Teskey, 2004). This spine density included 0.65 ± 0.03 pedunculated spines/μm and 0.43 ± 0.02 non-pedunculated spines/μm. Following LFPI, the spine density of these dendrites did not differ significantly from controls ($p > 0.05$). However, basilar spine density did change significantly across time points after LFPI, as summarized below. Micrographs of representative dendrites from ipsilateral neocortex$_{II,III}$ are also provided (Supplementary Fig. 1; see online supplementary material at http://www.liebertonline.com).

From 1 h to 24 h post-LFPI in ipsilateral neocortex$_{II,III}$ the total spine density of basilar dendrites decreased by 27% (1 h post-LFPI versus 24 h post-LFPI, $p < 0.001$; Fig. 5A). Further analysis revealed an underlying 35% decrease in pedunculated spine density (1 h post-LFPI versus 24 h post-LFPI, $p < 0.01$; Fig. 5B), but no change in non-pedunculated spine density (1 h post-LFPI versus 24 h post-LFPI, $p > 0.05$; Fig. 5C), across these time points. In the contralateral hemisphere, a similar pattern was observed. From 1 h to 24 h post-LFPI in contralateral neocortex$_{II,III}$, basilar dendrites showed a 26% decrease in pedunculated spine density (1 h post-LFPI versus 24 h post-LFPI, $p < 0.001$; Fig. 5B), while non-pedunculated spine density was relatively unchanged ($p > 0.05$ versus control; Fig. 5C). Thus, the data demonstrate that from 1 h to 24 h post-LFPI basilar dendrites undergo a selective loss of pedunculated spine density in the bilateral neocortex$_{II,III}$.

The decrease in basilar spine density was followed by an increase. From 24 h to 1 week post-LFPI, basilar spine density increased by 35% in the ipsilateral neocortex$_{II,III}$, and by 26% in the contralateral neocortex$_{II,III}$ (24 h post-LFPI versus 1 week post-LFPI, $p < 0.01$; Fig. 5A). Again, the underlying change was in pedunculated spine density, which increased by 46% in the ipsilateral neocortex$_{II,III}$, and by 32% in the contralateral neocortex$_{II,III}$ across these time points (24 h post-LFPI versus 1 week post-LFPI, $p < 0.001$ and $p < 0.01$, respectively; Fig. 5B). The non-pedunculated spine density of basilar dendrites did not change from 24 h to 1 week post-LFPI, however, but did increase significantly from 1 h to 1 week post-LFPI in the contralateral neocortex$_{II,III}$ (1 h post-LFPI versus 1 week post-LFPI, $p < 0.05$; Fig. 5C). These data suggest extensive remodeling of basilar dendritic structure in the bilateral neocortex$_{II,III}$ during recovery from LFPI.

On apical dendrites in hippocampal CA1, lateral fluid percussion injury caused a delayed increase in spine density

CA1 pyramidal cells have proximal dendrites which form spine synapses primarily with Shaffer collateral and commissural axons (Spruston and McBain, 2007). In the rat brain, these synapses occur throughout the proximal apical and basilar dendritic arbors of CA1 pyramidal cells (Spruston and McBain, 2007). We investigated the effect of TBI on the spine density of these dendrites, beginning with the apical dendrites. In control brains, the proximal apical dendrites of CA1 pyramidals ($n = 15$) exhibited 1.56 ± 0.08 dendritic spines/μm,

consistent with previously published studies (Ruan et al., 2009; Schwarzbach et al., 2006). This spine density consisted of 0.83 ± 0.04 pedunculated spines/μm and 0.52 ± 0.05 non-pedunculated spines/μm. Similar to dendrites in neocortex$_{II,III}$, apical dendritic spine density was not affected at 1 h post-LFPI, in either hemisphere of CA1 ($p > 0.05$ versus control; Fig. 6A–C). Nor was there any appreciable change in spine density by 24 h post-LFPI ($p > 0.05$ versus control; Fig. 6A–C), in contrast to what was observed in neocortex$_{II,III}$. However, there was a delayed increase in the spine density of CA1 apical dendrites, as described below. Micrographs of representative dendrites from ipsilateral CA1 are provided as a supplementary figure (Supplementary Fig. 2; see online supplementary material at http://www.liebertonline.com).

By 1 week post-LFPI, the spine density of proximal apical dendrites increased dramatically in both hemispheres of CA1. In ipsilateral CA1, for instance, the spine density of these dendrites rose by 32% relative to controls ($p < 0.001$ versus control; Fig. 6A). Further analysis revealed underlying changes in pedunculated and non-pedunculated spine density, which increased by 31% and 33% respectively, compared to controls ($p < 0.001$ and 0.01 versus control, respectively; Fig. 6B and C). Meanwhile, in the contralateral CA1, spine density increased by 22% relative to controls ($p < 0.05$ versus control; Fig. 6A), though pedunculated and non-pedunculated spine density did not differ significantly from that of controls ($p > 0.05$ each versus control; Fig. 6B and C). Overall, the data indicate that LFPI causes a delayed, but substantial increase in the spine density of proximal apical dendrites in bilateral CA1. These changes are consistent with an increased density of excitatory synapses on CA1 dendrites (e.g., reactive synaptogenesis; Anderson et al., 1986; Esclapez et al., 1999), and so could have considerable implications for hippocampal circuitry in the injured brain.

On basilar dendrites in hippocampal CA1, lateral fluid percussion injury caused a delayed increase in spine density

Proximal basilar dendrites of CA1 pyramidals were also examined. In control brains, the proximal basilar dendrites of CA1 pyramidals ($n = 12$) exhibited 1.48 ± 0.11 spines/μm, similar to previously published data (Ruan et al., 2009). This total spine density included 0.92 ± 0.08 pedunculated spines/μm and 0.56 ± 0.04 non-pedunculated spines/μm. As with CA1 apical dendrites, the spine density of CA1 basilar dendrites at 1 h or 24 h post-LFPI did not differ significantly from

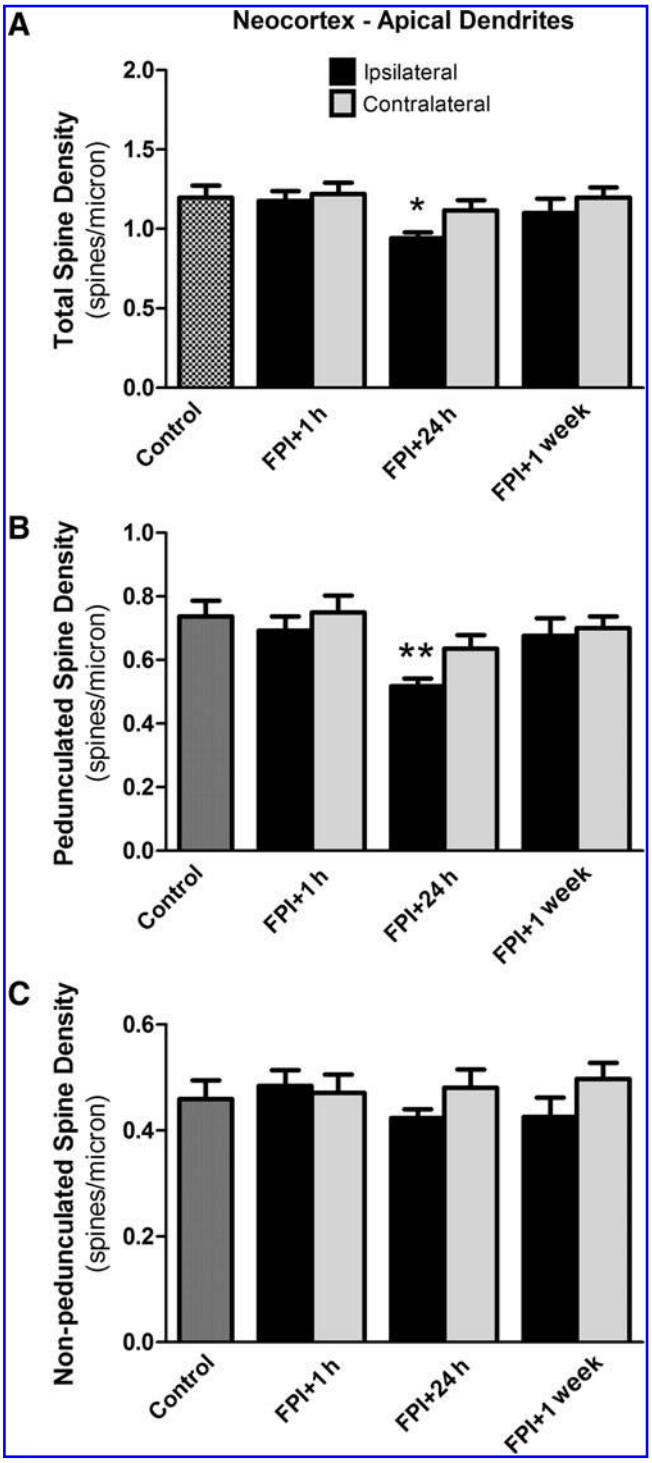

FIG. 4. On apical dendrites in neocortex$_{II,III}$, lateral fluid percussion injury caused a transient decrease in spine density. Rat brains were recovered 1 h, 24 h, or 1 week after moderate lateral fluid percussion injury (LFPI), and subjected to Golgi-Cox histochemistry. Golgi-stained pyramidal neurons were selected at random from neocortex layer II,III ("neocortex$_{II,III}$"), either adjacent to the site of injury ("ipsilateral"; black bars), or in an analogous region of the contralateral hemisphere ("contralateral"; gray bars). The density of pedunculated spines (mushroom spines and thin spines), and the density of non-pedunculated spines (stubby spines and filopodia-like spines) were each quantified on traced segments of proximal apical dendrites ($n_{neurons} > 13$). In ipsilateral neocortex$_{II,III}$, apical dendritic spine density decreased significantly by 24 h post-LFPI, relative to controls (**A**). Further analysis revealed a phenotype-specific change in spine density, specifically, a decrease in the density of pedunculated spines (**B**), with no appreciable change in the density of non-pedunculated spines (**C**). Both total and pedunculated spine densities recovered by 1 week post-LFPI (**A** and **B**). Meanwhile, in contralateral neocortex$_{II,III}$, the spine density of apical dendrites did not differ significantly from that of controls at any time point (**B**; $^{*}p < 0.05$ versus control; $^{**}p < 0.01$ versus control).

that of controls ($p > 0.05$ ipsilateral or contralateral versus control; Fig. 7A–C).

By 1 week post-LFPI, however, basilar dendrites in both hemispheres of CA1 showed significant increases in spine density. In ipsilateral CA1 for example, spine density increased 23% relative to controls (1.82 ± 0.08 total spines/μm versus control, $p < 0.01$; Fig. 7A), though neither pedunculated nor non-pedunculated spine density at 1 week post-LFPI differed significantly from controls ($p > 0.05$ each versus control; Fig. 7B and C). However, the pedunculated spine density at this time point was increased when compared to earlier time points, by 33% relative to 1 h post-LFPI and by 49% relative to 24 h post-LFPI (1 h post-LFPI versus 1 week post-LFPI, $p < 0.01$; 24 h post-LFPI versus 1 week post-LFPI, $p < 0.001$; Fig. 7B).

Meanwhile, in the contralateral CA1, a similar increase in spine density was observed. Basilar dendrites in contralateral CA1 showed a 27% increase in total spine density ($p < 0.05$ versus control; Fig. 7A), apparently driven by a 25% rise in pedunculated spine density ($p < 0.05$ versus control; Fig. 7B). Therefore, the data indicate that LFPI causes a delayed, but significant increase in basilar dendritic spine density bilaterally in CA1. As with the apical dendrites in CA1, this increase in spine density could signify the formation of novel excitatory circuits in the injured brain.

On apical dendrites in hippocampal CA3, lateral fluid percussion injury caused a delayed increase in spine density

Pyramidal cells of hippocampal CA3 form synapses with associational and commissural fibers on dendritic spines throughout their proximal apical and basilar arbors (Spruston and McBain, 2007). To understand the effect of LFPI on these spines, we compared apical dendritic spine density between control and laterally-injured brains. In control brains, the proximal apical dendrites of CA3 pyramidals ($n = 10$) averaged 1.24 ± 0.11 dendritic spines/μm, comprising 0.72 ± 0.08 pedunculated spines/μm and 0.52 ± 0.04 non-pedunculated spines/μm. Similarly to what was observed in CA1, apical dendritic spine density at 1 h or 24 h post-LFPI did not differ

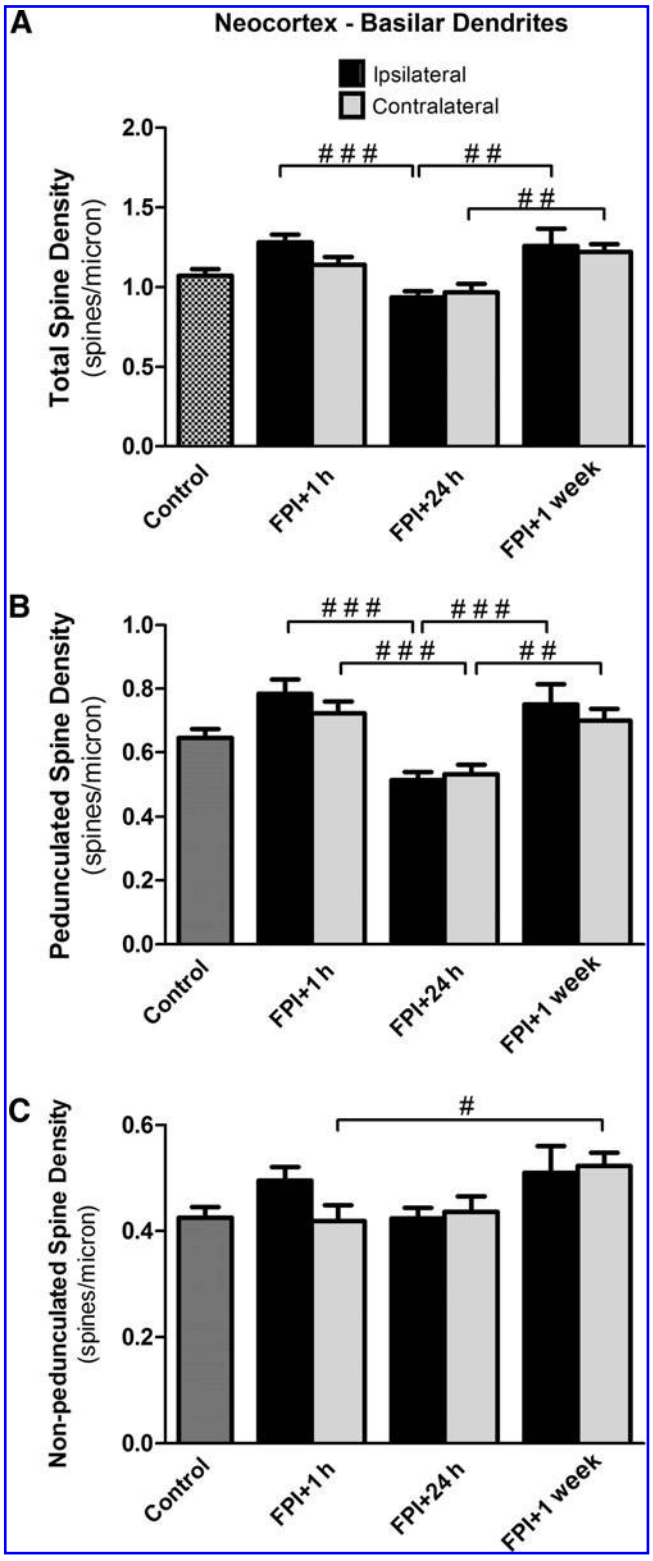

FIG. 5. On basilar dendrites in neocortex$_{II,III}$, spine density fluctuated during recovery from lateral fluid percussion injury (LFPI). Rat brains were recovered 1 h, 24 h, or 1 week after moderate lateral fluid percussion injury and stained using a Golgi-Cox procedure. Golgi-stained pyramidal neurons were selected at random from neocortex layer II,III ("neocortex$_{II,III}$"), either adjacent to the site of injury ("ipsilateral"; black bars) or in an analogous region of the contralateral hemisphere ("contralateral"; gray bars). Pedunculated spine density (mushroom spines and thin spines) and non-pedunculated spine density (stubby spines and filopodia-like spines) were quantified on traced segments of proximal basilar dendrites ($n_{neurons} > 13$). The spine density of these dendrites did not change relative to controls, but showed significant changes across time points post-LFPI. For example, the total spine density of these dendrites decreased from 1 h to 24 h post-LFPI in ipsilateral neocortex$_{II,III}$, and increased from 24 h to 1 week post-LFPI in bilateral neocortex$_{II,III}$ (**A**). Further analysis revealed underlying changes in pedunculated spine density, which decreased from 1 h to 24 h post-LFPI and increased from 24 h to 1 week post-LFPI, in both hemispheres of neocortex$_{II,III}$ (**B**). However, there were no corresponding changes in non-pedunculated spine density, except an increase from 1 h to 1 week post-LFPI in the contralateral neocortex$_{II,III}$ (**C**; #$p < 0.05$ versus other bracketed group; ##$p < 0.01$ versus other bracketed group; ### $p < 0.01$ versus other bracketed group).

significantly from that of controls, in either hemisphere of CA3 ($p > 0.05$ versus control; Fig. 8A–C).

As was also observed in CA1, however, LFPI caused a delayed increase in the spine density of apical CA3 dendrites. By 1 week post-LFPI in ipsilateral CA3, for instance, spine density increased 31% relative to controls ($p < 0.01$ versus control; Fig. 8A). Further analysis revealed an underlying, 33% increase in pedunculated spine density ($p < 0.05$ versus control; Fig. 8B), but no significant change in non-pedunculated spine density ($p > 0.05$ versus control; Fig. 8C), relative to controls. However, unlike what was observed in CA1, the effect appeared to be limited to the ipsilateral hemisphere: in the contralateral CA3, spine density at 1 week post-LFPI did not differ significantly from that of controls ($p > 0.05$ versus control; Fig. 8A–C), though pedunculated spine density had increased 44% relative to the 24 h post-LFPI time point (24 h post-LFPI versus 1 week post-LFPI, $p < 0.05$; Fig. 8B). Therefore, LFPI caused a delayed increase in the spine density of CA3 apical dendrites, and to a greater extent in the ipsilateral hemisphere. As with the neocortex and CA1, this increase in spine density could have substantial implications for the excitatory circuitry of the injured forebrain.

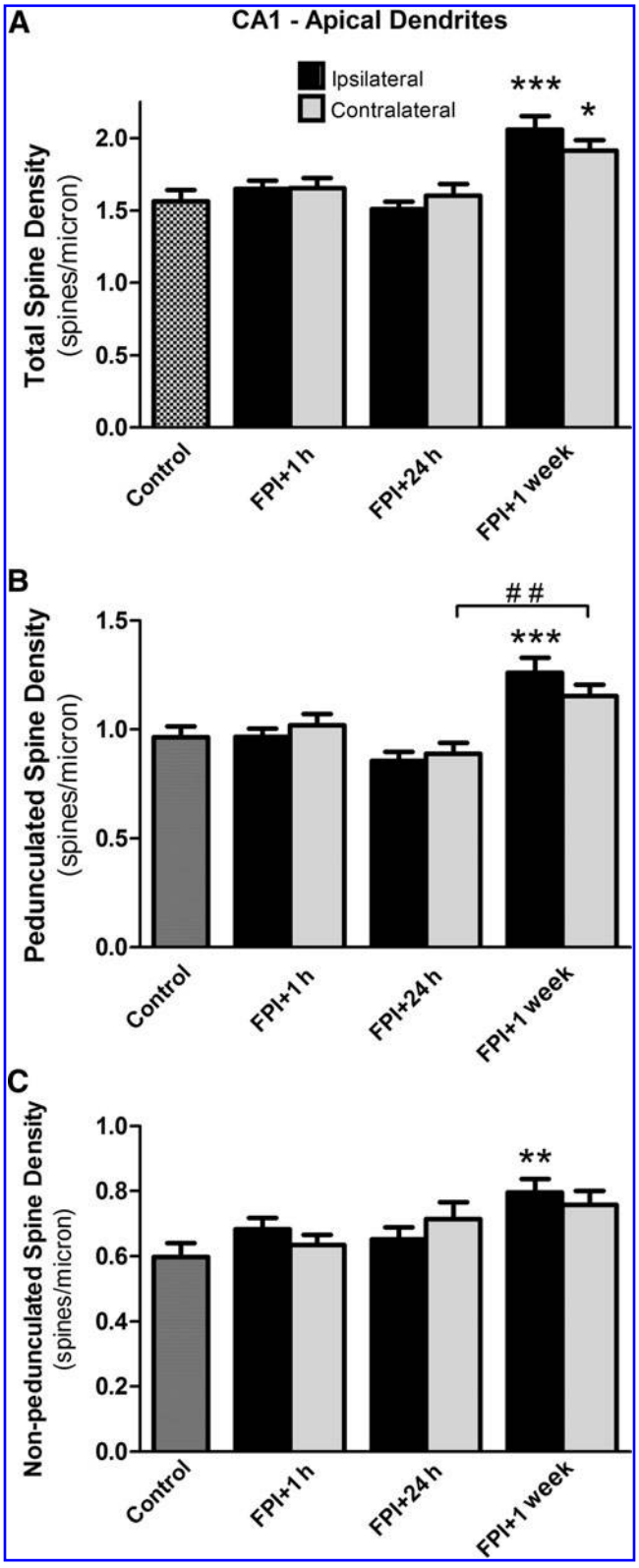

On basilar dendrites in hippocampal CA3, lateral fluid percussion injury caused a delayed increase in spine density

Basilar dendrites of CA3 pyramidal cells were also examined in control and laterally-injured brains. In control brains, the proximal basilar dendrites of CA3 pyramidals ($n = 12$) exhibited 1.28 ± 0.09 dendritic spines/μm, which consisted of 0.73 ± 0.05 pedunculated spines/μm and 0.55 ± 0.04 non-pedunculated spines/μm. Consistent with the apical dendrites in this region, the spine density of basilar dendrites at 1 h or 24 h post-LFPI did not differ significantly from that of controls, in either hemisphere of CA3 ($p < 0.05$ versus control; Fig. 9A–C). However, these dendrites also showed a delayed increase in spine density, as described below. Micrographs of representative dendrites from ipsilateral CA3 are provided as a supplementary figure (Supplementary Fig. 3; see online supplementary material at http://www.liebertonline.com).

By 1 week post-LFPI, the spine density of CA3 basilar dendrites increased significantly above control levels in both hemispheres. In the ipsilateral CA3, for example, these dendrites showed a 34% increase in total spine density, driven by a 41% increase in pedunculated spine density ($p < 0.01$ each

FIG. 6. On apical dendrites in hippocampal CA1, lateral fluid percussion injury (LFPI) caused a delayed increase in spine density. Rat brains were recovered 1 h, 24 h, or 1 week after moderate lateral fluid percussion injury and subjected to Golgi-Cox histochemistry. Golgi-stained pyramidal neurons were selected at random from ipsilateral CA1 (black bars) and from contralateral CA1 (gray bars) regions. Pedunculated spine density (mushroom spines and thin spines) and non-pedunculated spine density (stubby spines and filopodia-like spines) were quantified on traced segments of proximal apical dendrites ($n_{neurons} > 13$). The total spine density of these dendrites increased significantly at 1 week post-LFPI relative to controls, in both hemispheres of CA1 (**A**). Pedunculated spine density increased significantly at 1 week post-LFPI relative to controls in ipsilateral CA1, and from 24 h to 1 week post-LFPI in contralateral CA1 (**B**). In addition, ipsilateral CA1 showed a corresponding increase in non-pedunculated spine density at 1 week post-LFPI (**C**; $^*p < 0.05$ versus control; $^{**}p < 0.01$ versus control; $^{***}p < 0.001$ versus control; $\#\#p < 0.01$ versus other bracketed group).

versus control; Fig. 9B). While non-pedunculated spine density at 1 week post-LFPI did not change significantly relative to controls, it did increase by 66% from 1 h post-LFPI and by 27% from 24 h post-LFPI (1 h post-LFPI versus 1 week post-LFPI, $p < 0.001$; 24 h post-LFPI versus 1 week post-LFPI, $p < 0.05$; Fig. 9C). Meanwhile, in the contralateral CA3, similar changes in spine density were observed: total spine density increased by 25%, driven by a 36% increase in pedunculated spine density, compared to controls ($p < 0.05$ and $p < 0.01$ versus control, respectively; Fig. 9B).

In general, the data indicate that LFPI caused a delayed increase in basilar spine density in both hemispheres of CA3. As with neocortex$_{II,III}$ and CA1, this increase in spine density could indicate an increased density of excitatory synapses and therefore have considerable implications for hippocampal circuitry in the injured brain.

On dentate granule cell dendrites, lateral fluid percussion injury caused an acute decrease and a delayed increase in spine density

Granule cells, the principal cells of the dentate gyrus, receive mostly associational and commissural synapses on spines of their proximal dendrites (Spruston and McBain, 2007). The spine density of these dendrites in the dorsal dentate gyrus (dDG) was compared between control and laterally-injured brains. In control brains, the proximal dendrites of dDG granule cells ($n = 27$) displayed 1.43 ± 0.06 total spines/μm, as previously reported (Isokawa, 2000). This spine density included 0.83 ± 0.04 pedunculated spines/μm and 0.60 ± 0.03 non-pedunculated spines/μm. At 1 h after LFPI, the spine density of these dendrites was relatively unchanged in either hemisphere, relative to controls ($p > 0.05$ versus control; Fig. 10A–C). However, LFPI did cause a loss and subsequent gain of spine density in dDG at later time points, as described below. Micrographs of representative dendrites from ipsilateral dDG are provided as a supplementary figure (Supplementary Fig. 4; see online supplementary material at http://www.liebertonline.com).

By 24 h post-LFPI, dDG showed a hemisphere-specific loss of spine density. Specifically, in the ipsilateral dDG, pedunculated spine density decreased 20% ($p < 0.05$ versus control; Fig. 10B), without any appreciable change in non-pedunculated spine density ($p > 0.05$ versus control; Fig. 10C), relative to controls. However, in the contralateral dDG, spine density at 24 h post-LFPI did not differ significantly from that of controls ($p > 0.05$ versus control; Fig. 10A–C).

As observed in neocortex$_{II/II}$, the loss of spine density in dDG was not permanent. In fact, by 1 week post-LFPI, spine

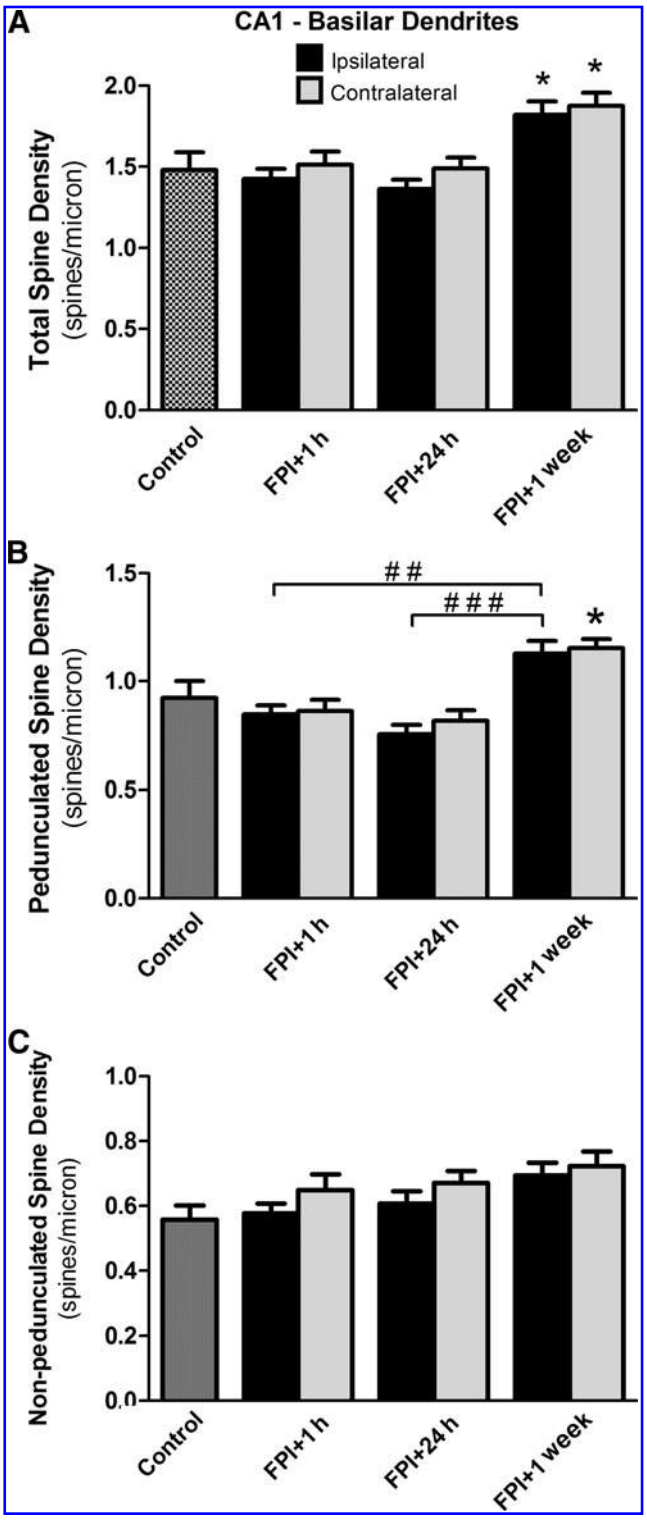

FIG. 7. On basilar dendrites in hippocampal CA1, lateral fluid percussion injury (LFPI) caused a delayed increase in spine density. Rat brains were recovered 1 h, 24 h, or 1 week after moderate lateral fluid percussion injury and stained using a Golgi-Cox procedure. Golgi-stained pyramidal neurons were selected at random from ipsilateral CA1 (black bars) and from contralateral CA1 (gray bars). Pedunculated spine density (mushroom spines and thin spines) and non-pedunculated spine density (stubby spines and filopodia-like spines) were quantified on traced segments of proximal basilar dendrites ($n_{neurons} > 12$). The total spine density of these dendrites increased significantly at 1 week post-LFPI relative to controls, in both hemispheres of CA1 (**A**). Pedunculated spine density increased significantly from 1 h to 1 week post-LFPI and from 24 h to 1 week post-LFPI in ipsilateral CA1, and relative to controls in contralateral CA1 (**B**). However, there were no corresponding changes in the non-pedunculated spine density of these dendrites (**C**; $*p < 0.05$ versus control; $\#\#p < 0.01$ versus other bracketed group; $\#\#\#p < 0.001$ versus other bracketed group).

density in the ipsilateral dDG had increased above control levels. In particular, total spine density increased 17% over control values ($p < 0.05$ versus control; Fig. 10A), apparently driven by an 18% rise in pedunculated spine density relative to controls ($p < 0.05$ versus control; Fig. 10B). While the non-pedunculated spine density of these dendrites did not change relative to controls ($p > 0.05$ versus control; Fig. 10C), it did increase 20% relative to the 1 h and 24 h post-LFPI time points (1 h post-LFPI versus 1 week post-LFPI, $p < 0.05$; 24 h post-LFPI versus 1 week post-LFPI, $p < 0.05$; Fig. 10C).

In the contralateral dDG, spine density also increased at 1 week post-LFPI, but only when compared to earlier post-LFPI time points. For example, total spine density in the contralateral dDG increased 22% from 1 h post-LFPI and 23% from 24 h post-LFPI (1 h post-LFPI versus 1 week post-LFPI, $p < 0.05$; 24 h post-LFPI versus 1 week post-LFPI, $p < 0.05$; Fig. 10A). Likewise, pedunculated spine density in the contralateral dDG increased 26% from 1 h post-LFPI and 43% from 24 h post-LFPI (1 h post-LFPI versus 1 week post-LFPI, $p < 0.05$; 24 h post-LFPI versus 1 week post-LFPI, $p < 0.001$; Fig. 10B). However, non-pedunculated spine density at this time point did not differ significantly from controls nor from earlier post-LFPI time points (versus control, 24 h post-LFPI, or 1 h post-LFPI; $p > 0.05$; Fig. 10C). Overall, the data show that LFPI causes a delayed increase in the proximal dendritic spine density of granule cells in the ipsilateral dDG. This increase in spine density, like that observed in the other hippocampal subfields, may indicate substantial re-wiring of the hippocampus in response to lateral brain injury.

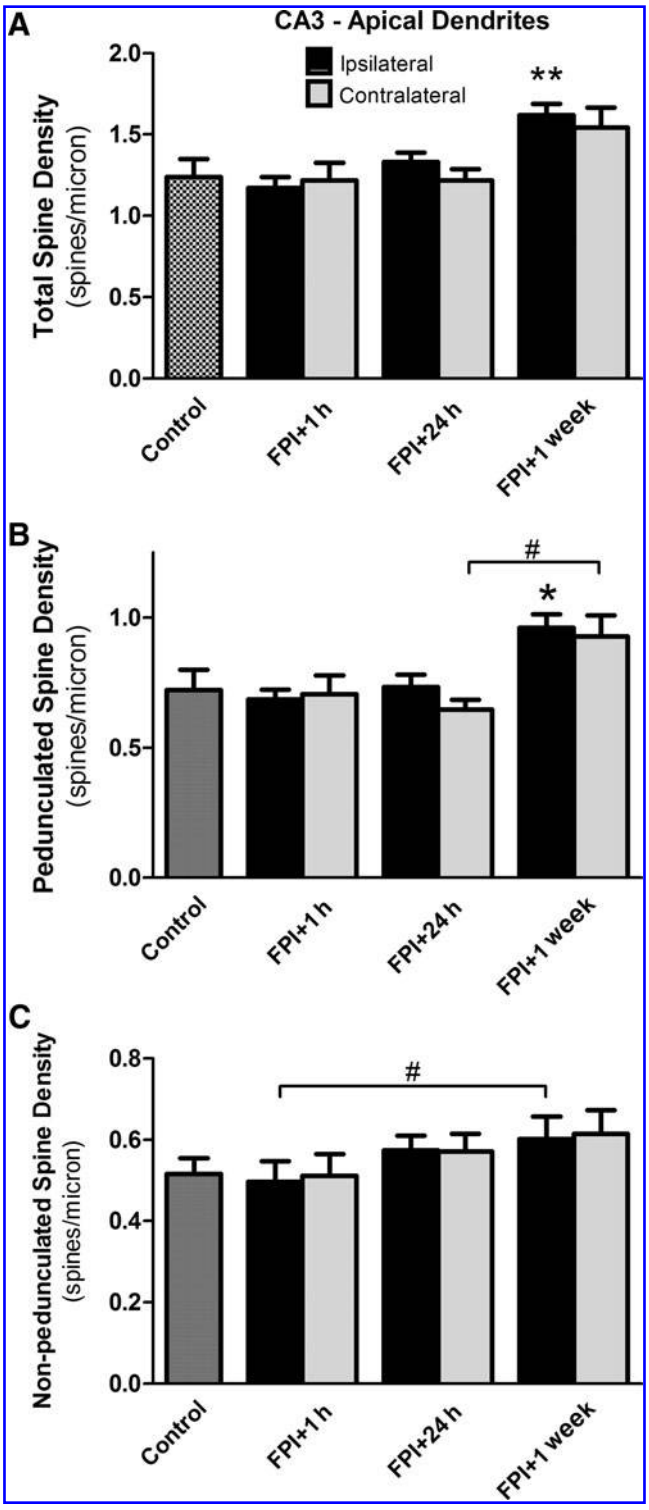

FK506 administration increased dendritic spine density in uninjured neocortex$_{II,III}$

In vivo imaging has revealed a daily turnover in dendritic spine populations of the adult rodent brain (Grutzendler et al., 2002; Xu et al., 2007). If this turnover of dendritic spines is mediated by CaN, then inhibiting CaN could increase the density of dendritic spines. To test this hypothesis and reduce a potential confound to the present study, uninjured subjects were administered the calcineurin inhibitor FK506 (5 mg/kg IP) and their brains were recovered 2 h or 23 h later for Golgi-Cox analysis of spine density. The mean spine densities ratio$_{P:N}$ are provided in Supplementary Table 1 (see online supplementary material at http://www.liebertonline.com).

FK506 administration caused significant increases in the pedunculated spine density of basilar dendrites in neocortex$_{II,III}$, relative to drug-naïve controls. Specifically, at 2 h post-injection, the pedunculated spine density of these dendrites increased 29% relative to drug-naïve controls ($p < 0.05$ versus

FIG. 8. On apical dendrites in hippocampal CA3, lateral fluid percussion injury (LFPI) caused a delayed increase in spine density. Rat brains were recovered 1 h, 24 h, or 1 week after moderate lateral fluid percussion injury and subjected to Golgi-Cox histochemistry. Golgi-stained pyramidal neurons were selected at random from ipsilateral CA3 (black bars) and from contralateral CA3 (gray bars). Pedunculated spine density (mushroom spines and thin spines) and non-pedunculated spine density (stubby spines and filopodia-like spines) were quantified on traced segments of proximal apical dendrites ($n_{neurons} > 10$). In ipsilateral CA3, the total spine density of these dendrites increased significantly at 1 week post-LFPI (**A**), driven by a rise in pedunculated spine density (**B**), relative to controls. In contrast, the contralateral CA3 showed only an increase in pedunculated spine density from 24 h to 1 week post-LFPI (**B**). In terms of non-pedunculated spine density, the only significant change was an increase from 1 h to 1 week post-LFPI in ipsilateral CA3 (**C**; $^*p < 0.05$ versus control; $^{**}p < 0.01$ versus control; $\#p < 0.05$ versus other bracketed group).

drug-naïve control; Fig. 11B). This increase appeared to persist for many hours. By 23 h post-injection, pedunculated spine density was increased 31% relative to drug-naïve controls, driving a significant 29% increase in the total spine density, relative to drug-naïve controls ($p < 0.001$ and 0.01 versus drug-naïve control, respectively; Fig. 11A and B). A similar effect was recently reported in adult mice given daily doses of FK506 (Spires-Jones et al., 2011), and another study found that CaN inhibition increases synaptogenesis (Schwartz et al., 2009). However, these findings are beyond the scope of the present study. Still, to avoid a potential confound to our study, FK506-treated, injured subjects were compared only to FK506-treated, uninjured subjects.

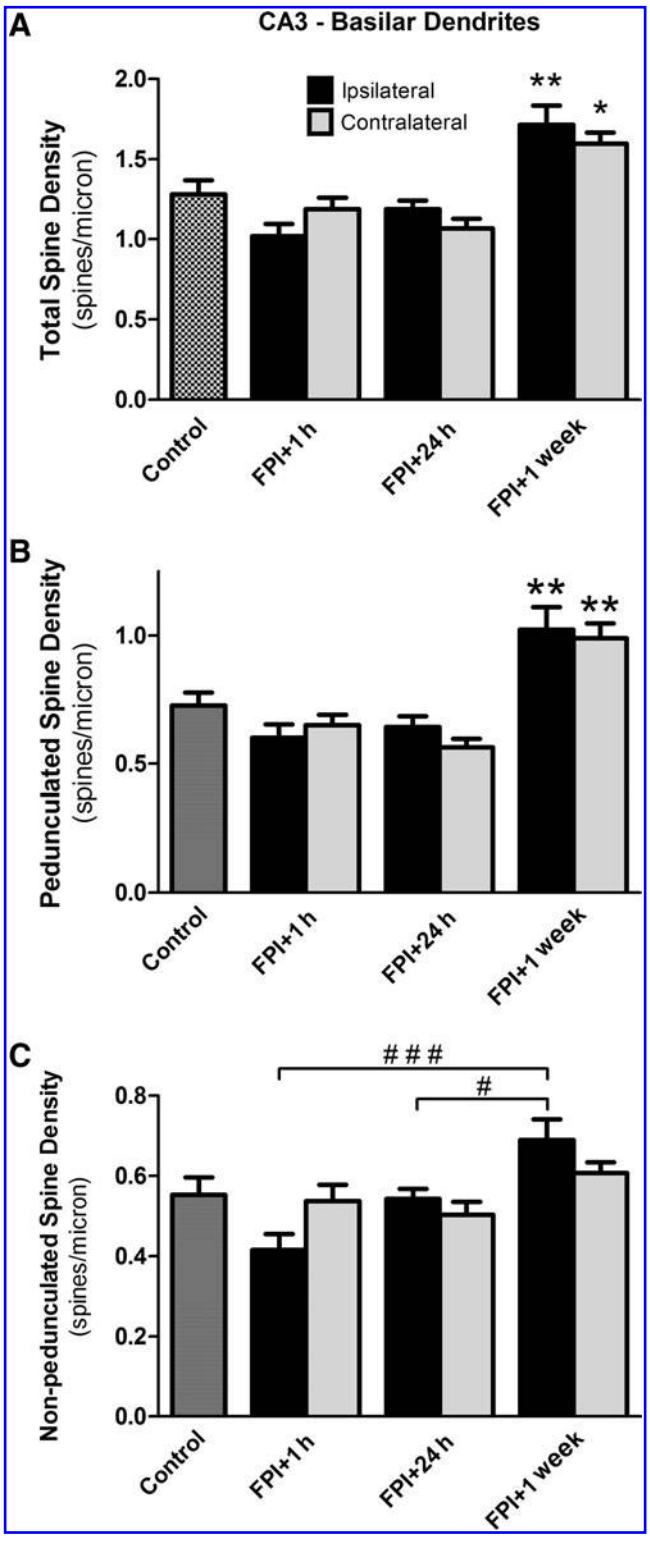

FK506 administration prevented the loss of dendritic spine density at 24 h post-injury

CaN activity has been implicated in the injury-induced loss of dendritic spine density *in vitro* (Halpain et al., 1998) and *in vivo* (Kurz et al., 2008; Zeng et al., 2007). To determine whether CaN activity could explain the loss of spine density at 24 h post-LFPI, some experimental subjects ($n = 3$) were administered the CaN inhibitor FK506 (5 mg/kg IP) 1 h after LFPI. The timing of this injection was based on evidence that CaN activity increases within hours of LFPI (Campbell et al., 2011). Furthermore, this dosage of FK506 has been shown to block dendritic spine loss in a different *in vivo* model of brain injury (Kurz et al., 2008). Brains of FK506-treated subjects were harvested 24 h after LFPI and subjected to Golgi-Cox histochemistry. Some uninjured subjects ($n = 3$) were used as drug controls and received a single injection of FK506 (5 mg/kg IP) 23 h prior to sacrifice.

A single, post-injury injection of FK506 completely blocked the decreases in spine density otherwise observed at 24 h post-LFPI. Indeed, spine density was not statistically significantly different between uninjured and injured subjects treated with FK506, in any region examined, on either apical or basilar dendrites ($p > 0.05$ each versus control; Fig. 12). This means that FK506 preserved spine density in those regions which otherwise lost roughly 20% of their spine density at this time point (i.e., ipsilateral neocortex$_{II,III}$ and dDG). These data thus strongly suggest that CaN activity is necessary for the loss of spine density at 24 h post-LFPI.

Discussion

This study demonstrates that LFPI can cause significant changes in dendritic spine density and that these changes are

FIG. 9. On basilar dendrites in hippocampal CA3, lateral fluid percussion injury (LFPI) caused an acute decrease and delayed increase in spine density. Rat brains were recovered 1 h, 24 h, or 1 week after moderate lateral fluid percussion injury and stained using a Golgi-Cox procedure. Golgi-stained pyramidal neurons were selected at random from ipsilateral CA3 (black bars) and from contralateral CA3 (gray bars). Pedunculated spine density (mushroom spines and thin spines) and non-pedunculated spine density (stubby spines and filopodia-like spines) were quantified on traced segments of proximal basilar dendrites ($n_{neurons} > 12$). The total spine density of these dendrites increased significantly by 1 week post-LFPI relative to controls, in both hemispheres of CA3 (**A**). Further analysis revealed underlying changes in pedunculated spine density, which increased significantly in both hemispheres of CA3 relative to controls (**B**). In contrast, non-pedunculated spine density did not change appreciably in either hemisphere of CA3 relative to controls, but did increase from 1 h to 1 week post-LFPI and from 1 h to 24 h post-LFPI in the ipsilateral CA3 (**C**; $*p < 0.05$ versus control; $**p < 0.01$ versus control; $\#p < 0.05$ versus other bracketed group; $\#\#\#p < 0.001$ versus other bracketed group).

time- and brain region-specific. One major finding is that LFPI caused a loss of spine density on proximal dendrites in ipsilateral neocortex$_{II,III}$ and dDG. This loss of spine density was prevented by administration of FK506, a pharmacological inhibitor of CaN, which represents a second major finding in this study. Indeed, a single, post-injury dose of FK506 preserved spine density at 24 h post-LFPI. A third major finding is that LFPI causes a delayed, regional increase in spine density in both hemispheres of rat hippocampus, which is consistent with reactive synaptogenesis (e.g., Anderson et al., 1986; Esclapez et al., 1999). Specifically, within 1 week of LFPI, spine density increased in CA1 and CA3 bilaterally, and in dDG ipsilaterally. The implications of each of these major findings are considered below.

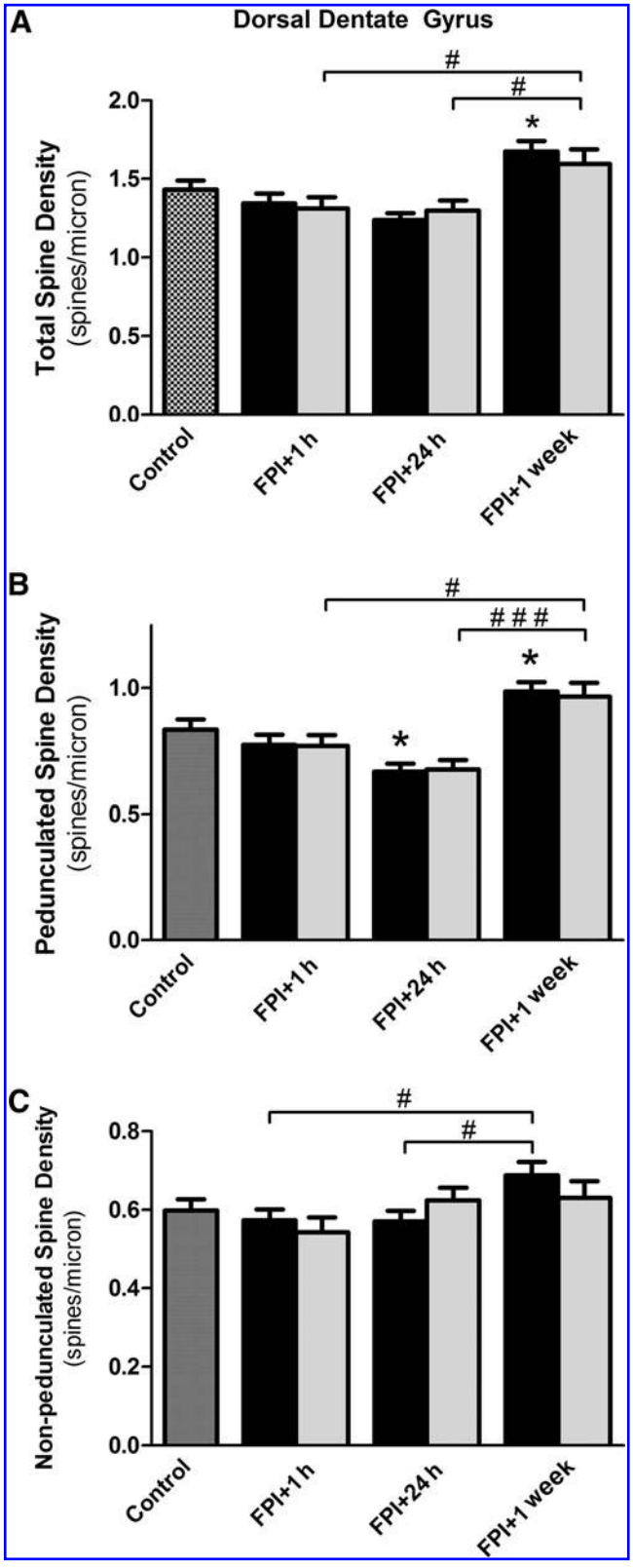

Lateral fluid percussion injury caused a loss of spine density in neocortex and dentate gyrus

In theory, a reduction in dendritic spine density could be due to a loss of spines or to a lengthening of the dendrite. Though the latter possibility cannot be excluded by this study, it seems unlikely for three reasons: first, a shortening, rather than a lengthening, of pyramidal dendrites has been reported in a lateral TBI model (Hoskison et al., 2009); second, *in vitro* imaging of developing neurons suggests that dendrites grow from the terminal tip or branch point (Wu et al., 1999), which would not affect the medial portion that we sampled for spine density; third, our data indicate that LFPI differentially affects pedunculated and non-pedunculated spine densities. For these reasons, a loss of spines most likely explains the reduction in spine density we observed. Interestingly, this spine loss corresponds in time, region, and magnitude with a loss of synaptic proteins reported in a different TBI model (Ansari et al., 2008). Taken together, these findings suggest that lateral TBI causes synapse degeneration near the site of focal injury.

Interestingly, the apparent loss of pedunculated spines we observed at 24 h post-LFPI occurred independent of any change in non-pedunculated spine density. There are a number of possible explanations for this phenotype-specific effect. One possibility relates to the mechanism of spine loss: if an excess (or lack) of synaptic activity caused the spine loss, only spines with synapses would be directly affected. Since

FIG. 10. On dentate granule cell dendrites, lateral fluid percussion injury caused an acute decrease and a delayed increase in spine density. Rat brains were recovered 1 h, 24 h, or 1 week after moderate lateral fluid percussion injury and subjected to Golgi-Cox histochemistry. Golgi-stained granule cells were selected at random from the dorsal leaf of the dentate gyrus (dDG) in the ipsilateral (black bars) and the contralateral (gray bars) hemispheres. Pedunculated spine density (mushroom spines and thin spines) and non-pedunculated spine density (stubby spines and filopodia-like spines) were quantified on traced segments of proximal dendrites ($n_{neurons} > 12$). The total spine density of these dendrites increased by 1 week post-LFPI relative to controls in the ipsilateral dDG, as well as from 1 h to 1 week and from 24 h to 1 week in the contralateral dDG (**A**). In terms of pedunculated spine density, the ipsilateral dDG showed a significant decrease at 24 h post-LFPI and a significant increase at 1 week post-LFPI, whereas the contralateral dDG showed an increase from 1 h to 1 week post-LFPI and from 24 h to 1 week post-LFPI (**B**). The non-pedunculated spine density of these dendrites only changed appreciably in the ipsilateral dDG, where an increase was observed from 1 h to 1 week post-LFPI and from 24 h to 1 week post-LFPI (**C**; $^*p < 0.05$ versus control; $\#p < 0.05$ versus other bracketed group; $\#\#\#p < 0.001$ versus other bracketed group).

the pedunculated phenotype is typical of synapse-bearing spines (Bourne and Harris, 2007), this can explain why only pedunculated spines were lost after LFPI.

An alternative explanation is that both spine populations decrease after LFPI, but only non-pedunculated spines are replenished by 24 h post-LFPI. Non-pedunculated spines could replenish in response to a decrease in synaptic activity after LFPI. Indeed, immature spines are formed in response to a pharmacological blockade of synaptic transmission in the hippocampus *in vitro* (Petrak et al., 2005); a similar effect could occur with a reduction in synaptic transmission, or with a loss of synapses (e.g., the 60% loss that occurs within days of lateral cortical contusion; Scheff et al., 2005).

A third possibility is that LFPI causes some pedunculated spines to shrink and assume a non-pedunculated morphology. Shrinkage of pedunculated spines could mask a loss of non-pedunculated spines. Indeed, spine shrinkage is associated with activation of the actin binding protein, cofilin (Zhou et al., 2004). Our companion study (Campbell et al., 2011) reports that cofilin activation in the neocortex and hippocampus coincides with the spine loss we observed. For these reasons, spine shrinkage could explain why only pedunculated spines appeared to be affected by LFPI. Future studies using *in vivo* imaging and transgenic techniques are needed to better characterize the fate of pedunculated and non-pedunculated spines in this brain injury model.

Further study is also needed to determine whether the spine loss we observed corresponds to a loss of synapses. Studies in which cultured neurons were exposed to glutamate receptor agonists (Halpain et al., 1998; Hasbani et al., 2001) or cold (Kirov et al., 2004) suggest that collapsed dendritic spines can maintain synaptic contacts. However, other *in vitro* studies show that spine collapse can disrupt synapses: in hippocampal slices, excessive synaptic activity leads to an FK506-sensitive upregulation of Snk (serum-inducible kinase), resulting in proteolysis of the spine-stabilizing protein, SPAR (spine-associated Rap guanosine triphosphatase activating protein; Pak and Sheng, 2003). This Snk-SPAR pathway leads to spine loss as well as reductions in miniature post-synaptic potentials and in the immunoreactivity of the critical post-synaptic protein, PSD-95 (Pak and Sheng, 2003; Seeburg and Sheng, 2008). Interestingly, the Snk-SPAR pathway primarily affects pedunculated spines on proximal dendrites (Pak and Sheng, 2003) and requires hours to develop (Seeburg and Sheng, 2008; Wu et al., 2007). These *in vitro* findings are therefore consistent with our observation that spine loss

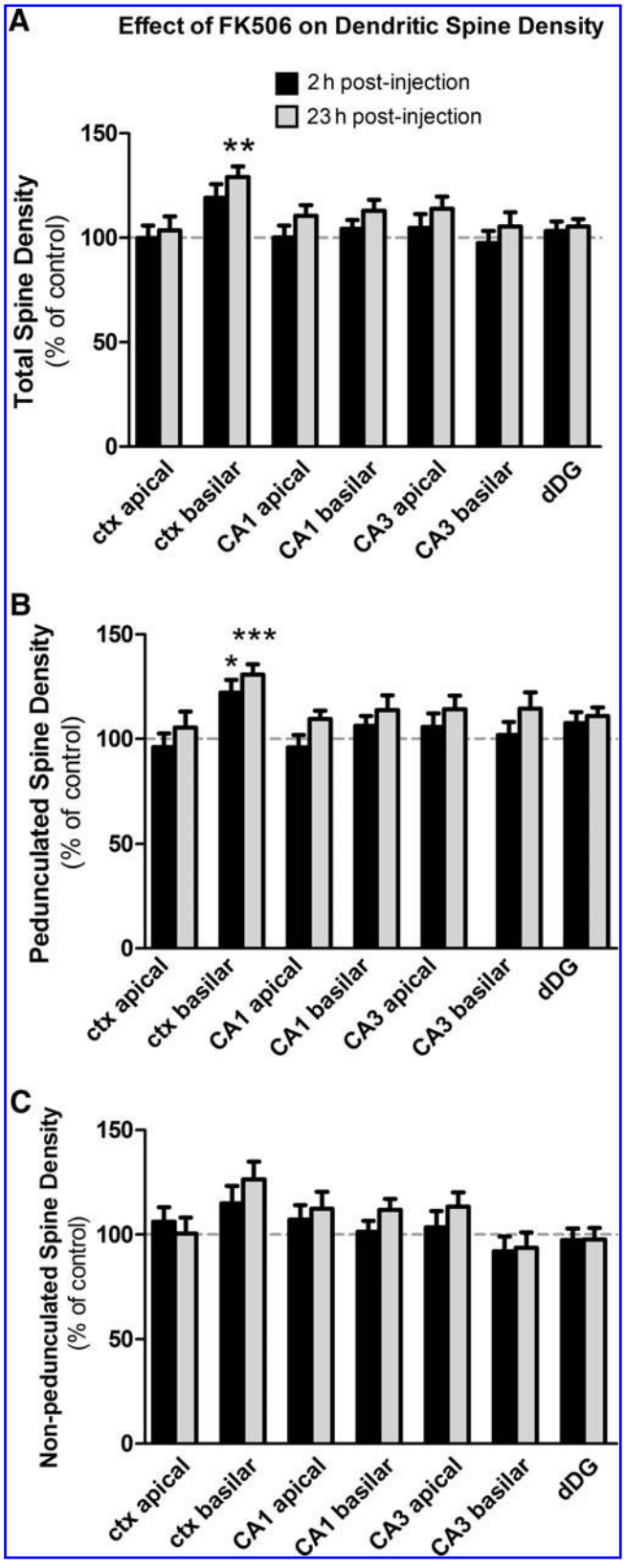

FIG. 11. FK506 administration increased dendritic spine density in uninjured neocortex$_{II,III}$. Rat brains were recovered 2 h (black bars) or 23 h (gray bars) after FK506 administration (5 mg/kg IP), and subjected to Golgi-Cox histochemistry. Golgi-stained principal cells were selected at random and bilaterally from the following forebrain regions: neocortex$_{II,III}$, hippocampus CA1, hippocampal CA3, and the dorsal leaf of the dentate gyrus (*n* values are given in Supplementary Table 1; see online supplementary material at http://www.liebertonline.com). Pedunculated spine density and non-pedunculated spine density were quantified on traced segments of proximal dendrites. By 2 h post-injection, FK506 administration did not significantly affect the total spine density (**A**) or non-pedunculated spine density (**C**) of these dendrites, but caused a significant increase in the pedunculated spine density of basilar dendrites in neocortex$_{II,III}$ (ctx) relative to controls (**B**). By 23 h post-injection, both the total spine density (**A**) and pedunculated spine density (**B**) of basilar dendrites in neocortex$_{II,III}$ were increased significantly relative to controls (*$p < 0.05$ versus control; **$p < 0.01$ versus control; ***$p < 0.001$ versus control).

occurred on proximal dendrites and can explain the delay in the onset of spine loss after brain injury. Furthermore, our companion study (Campbell et al., 2011) found a slight loss of SPAR immunoreactivity in the ipsilateral hippocampus at 18 h post-LFPI. This finding raises the possibility that SPAR proteolysis can explain the spine loss observed in the present study in the ipsilateral dentate gyrus. Therefore, the potential role of this FK506-sensitive signaling pathway in TBI-induced spine loss is an intriguing topic for further study.

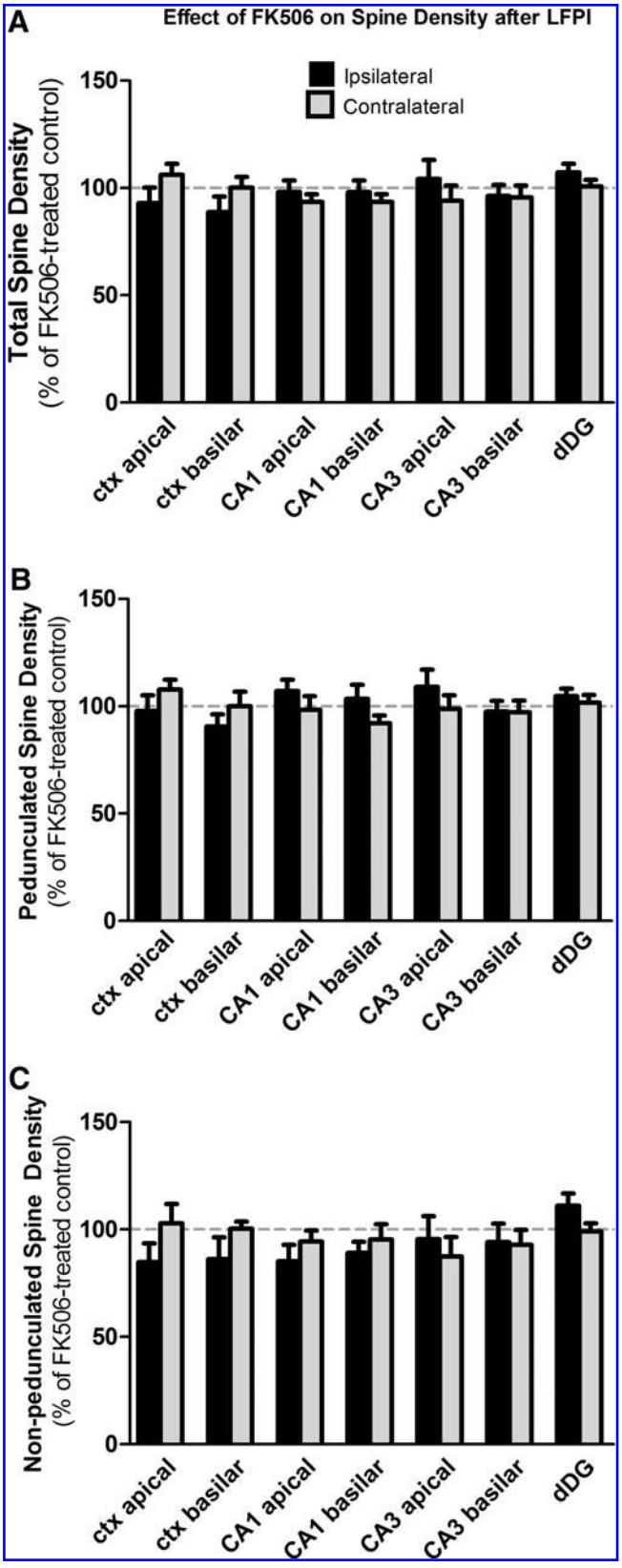

Pharmacological inhibition of calcineurin prevented the dendritic spine loss at 24 h post-injury

CaN is a calcium-stimulated phosphatase which mediates functional and structural plasticity on both sides of the synapse (Groth et al., 2003; Zhou et al., 2004). One mechanism by which CaN regulates post-synaptic structure involves the breakdown of the spine cytoskeleton. As demonstrated *in vitro*, CaN dephosphorylates and so activates Slingshot (Wang et al., 2005), a family of phosphatases which in turn activate proteins of the actin depolymerizing factor (ADF)/cofilin family (Niwa et al., 2002). Activated cofilin binds and breaks apart filaments of actin, enabling many forms of functional and structural plasticity in the neuron (for review, see Sarmiere and Bamburg, 2004). For example, cofilin is responsible for the shrinkage of dendritic spines that accompanies the long-term depression of spine synapses (Zhou et al., 2004).

Our companion study (Campbell et al., 2011) reports evidence that LFPI caused significant increases in cofilin activity. In some cases, the cofilin activation observed in our companion study corresponds to spine loss observed in the present study. Specifically, our companion study reports that the ipsilateral neocortex and hippocampus each show increases in cofilin activity at 24 h post-LFPI (signified by decreases in the phosphorylation of the cofilin serine 3 residue; Campbell et al., 2011). At the same time point and in the same forebrain regions, the present study reports a significant loss of dendritic spines. These parallel findings raise the possibility that cofilin activation is responsible for spine loss after LFPI (but see also Discussion in Campbell et al., 2011). Other brain injury models have also linked cofilin activation to spine loss (Kurz et al., 2008; Shankar et al., 2007; Zeng et al., 2007).

Another parallel between the present study and its companion involves the CaN inhibitor, FK506. Our companion study found that a single, post-injury injection of FK506

FIG. 12. FK506 administration prevented a loss of dendritic spine density following lateral fluid percussion injury (LFPI). Rats received a lateral brain injury by fluid percussion and were administered FK506 (5 mg/kg IP) 1 h later. Rat brains were recovered 24 h after injury and subjected to Golgi-Cox histochemistry. Golgi-stained principal cells were selected at random from the ipsilateral (black bars) and contralateral (gray bars) hemispheres of neocortex$_{II,III}$ (Ctx), hippocampus CA1, hippocampal CA3, and the dorsal leaf of the dentate gyrus (dDG; *n* values are provided in Supplementary Table 1; see online supplementary material at http://www.liebertonline.com). Pedunculated spine density and non-pedunculated spine density were quantified on proximal dendrites in these regions. Administering FK506 at 1 h post-injury did not affect non-pedunculated spine density (**C**) but preserved total spine density (**A**) and pedunculated spine density (**B**) at 24 h post-LFPI on apical dendrites in ipsilateral neocortex$_{II,III}$ and on granule cell dendrites in the ipsilateral dDG (**B**), dendrites which otherwise showed significant spine loss at this time point (see Fig. 4B and 10B). Data given as percent of FK506-treated, uninjured controls.

blocked cofilin de-phosphorylation in the neocortex at 24 h post-LFPI. At the same time point and in the same brain region, an identical FK506 treatment prevented spine loss in the present study. Therefore, in the neocortex at least, the FK506-sensitive de-phosphorylation of cofilin corresponds to spine loss after LFPI. These findings agree with our previous research in a rat model of status epilepticus, in which FK506 treatment (5 mg/kg) prevented cofilin de-phosphorylation and a coinciding loss of dendritic spines. Preventing spine loss in these different models of brain injury could maintain synaptic integrity and so reduce the risk of cognitive impairment and other sequelae. Therefore, these results emphasize the potential of CaN as a therapeutic target in treating brain injury.

Lateral fluid percussion injury caused a delayed overgrowth of dendritic spines in CA1, CA3, and dDG

Previously published studies do not predict an increase in dendritic spine density following lateral brain injury. For example, in a study by Schwarzbach and colleagues (2006), moderate (1.4–2.1 atm) lateral fluid percussion injury had no effect on the apical and basilar dendritic spine densities of mouse CA1 pyramidals at 1 week post-injury (Schwarzbach et al., 2006). In addition, Scheff and colleagues (2005) found that lateral cortical contusion caused a loss of synapses in CA1 stratum radiatum which lasted at least 60 days post-injury (Scheff et al., 2005). Consequently, though using a different model of TBI, we were surprised to find an increase in the dendritic spine density of CA1 apical dendrites (as well as in other brain regions) at 1 week post-LFPI.

It is possible that the spine overgrowth we observed in CA1 occurred only on proximal dendrites. Unlike previously published studies, our study focused on second- or third-order dendrites within 30–150 μm of the cell soma. Compared to distal dendrites, these proximal regions of CA1 pyramidal dendrites are less dense with synapses (Megias et al., 2001). Proximal dendrites may therefore be a more accessible target for re-innervating axons following injury. Indeed, the apical dendritic field of CA1, the stratum radiatum, is re-innervated within a week or so of lateral cortical contusion in rat (Norris and Scheff, 2009; Scheff et al., 2005). If re-innervating fibers connect with *de novo* dendritic spines, this could explain the increased spine density seen in CA1 at 1 week post-LFPI.

Delayed increases in spine density have also been associated with experimental denervation (Cesa et al., 2005) and ischemia. Within days of ischemic injury, for example, CA1 apical dendrites show an increase in spine density (Corbett et al., 2006; Ruan et al., 2009). Since moderate LFPI can depress cerebral blood flow (Dietrich et al., 1998), further investigation is needed to know whether there is a mechanistic relationship between spine overgrowth in the ischemia and LFPI models.

An overgrowth of dendritic spines may be a clue to understanding the altered electrophysiology of the hippocampus following lateral brain injury. An electrophysiological study by Akasu and colleagues found an increase in the excitability of rat CA1 at 1 week after moderate LFPI (1.5–2.0 atm; Akasu et al., 2002). Other research suggests that this increased excitability is due to recurrent circuits formed by CA1 axon collaterals. Indeed, CA1 axons invade the stratum radiatum within weeks of epileptogenic brain injury in rat, and this corresponds to an increase in CA1 excitability (Esclapez et al., 1999). It is likely that these CA1 axons form synapses on CA1 dendrites, since CA1 pyramidals become increasingly interconnected when brain injury leads to epilepsy (Shao and Dudek, 2005). Alternatively, the increased spine density in CA1 and CA3 may represent innervation by commissural or extra-hippocampal regions. In any case, further investigation is needed to determine whether reactive synaptogenesis can explain the spine overgrowth we observed. A better understanding of how the brain is re-wired after injury holds promise for the treatment of TBI-related pathologies such as cognitive impairment and post-traumatic epilepsy.

Acknowledgments

This research was funded by a grant from the Commonwealth Neurotrauma Initiative (#07-302E) to S.B.C. The authors gratefully acknowledge Dr. Robert Hamm for the use of the fluid percussion injury device, Dr. M. Alex Meredith for the use of the microscope and Neurolucida system, and Dr. John Povlishock for the use of the vibratome.

Author Disclosure Statement

No competing financial interests exist.

References

Akasu, T., Muraoka, N., and Hasuo, H. (2002). Hyperexcitability of hippocampal CA1 neurons after fluid percussion injury of the rat cerebral cortex. Neurosci. Lett. 329, 305–308.

Anderson, K.J., Scheff, S.W., and DeKosky, S.T. (1986). Reactive synaptogenesis in hippocampal area CA1 of aged and young adult rats. J. Comp. Neurol. 252, 374–384.

Ansari, M.A., Roberts, K.N., and Scheff, S.W. (2008). A time course of contusion-induced oxidative stress and synaptic proteins in cortex in a rat model of TBI. J. Neurotrauma 25, 513–526.

Bourne, J., and Harris, K.M. (2007). Do thin spines learn to be mushroom spines that remember? Curr. Opin. Neurobiol. 17, 381–386.

Campbell, J.N., Kurz, J.E., and Churn, S.B. (2009). Pathological remodeling of dendritic spines, in: *Dendritic Spines: Biochemistry, Modeling and Properties*. L.R. Baylog (ed). Nova Science Publishers: New York, pps. 45–66.

Campbell, J.N., Register, D.L., and Churn, S.B. (2011). Mechanisms of dendritic spine remodeling in a rat model of traumatic brain injury. J. Neurotrauma (Epub ahead of print).

Cesa, R., Morando, L., and Strata, P. (2005). Purkinje cell spinogenesis during architectural rewiring in the mature cerebellum. Eur. J. Neurosci. 22, 579–586.

Choi, D.W. (1992). Excitotoxic cell death. J. Neurobiol. 23, 1261–1276.

Corbett, D., Giles, T., Evans, S., McLean, J., and Biernaskie, J. (2006). Dynamic changes in CA1 dendritic spines associated with ischemic tolerance. Exp. Neurol. 202, 133–138.

Dietrich, W.D., Alonso, O., Busto, R., Prado, R., Zhao, W., Dewanjee, M.K., and Ginsberg, M.D. (1998). Posttraumatic cerebral ischemia after fluid percussion brain injury: an autoradiographic and histopathological study in rats. Neurosurgery 43, 585–593; discussion 593–584.

Dixon, C.E., Lyeth, B.G., Povlishock, J.T., Findling, R.L., Hamm, R.J., Marmarou, A., Young, H.F., and Hayes, R.L. (1987). A fluid percussion model of experimental brain injury in the rat. J. Neurosurg. 67, 110–119.

Esclapez, M., Hirsch, J.C., Ben-Ari, Y., and Bernard, C. (1999). Newly formed excitatory pathways provide a substrate for hyperexcitability in experimental temporal lobe epilepsy. J. Comp. Neurol. 408, 449–460.

Fiala, J.C., Spacek, J., and Harris, K.M. (2008). Dendrite structure, in: *Dendrites*, 2nd ed. G. Stuart, N. Spruston, and M. Häusser (eds). Oxford University Press: Oxford, pps. 1–41.

Groth, R.D., Dunbar, R.L., and Mermelstein, P.G. (2003). Calcineurin regulation of neuronal plasticity. Biochem. Biophys. Res. Commun. 311, 1159–1171.

Grutzendler, J., Kasthuri, N., and Gan, W.B. (2002). Long-term dendritic spine stability in the adult cortex. Nature 420, 812–816.

Halpain, S., Girault, J.A., and Greengard, P. (1990). Activation of NMDA receptors induces dephosphorylation of DARPP-32 in rat striatal slices. Nature 343, 369–372.

Halpain, S., Hipolito, A., and Saffer, L. (1998). Regulation of F-actin stability in dendritic spines by glutamate receptors and calcineurin. J. Neurosci. 18, 9835–9844.

Hasbani, M.J., Schlief, M.L., Fisher, D.A., and Goldberg, M.P. (2001). Dendritic spines lost during glutamate receptor activation reemerge at original sites of synaptic contact. J. Neurosci. 21, 2393–2403.

Hoskison, M.M., Moore, A.N., Hu, B., Orsi, S., Kobori, N., and Dash, P.K. (2009). Persistent working memory dysfunction following traumatic brain injury: Evidence for a time-dependent mechanism. Neuroscience 159, 483–491.

Isokawa, M. (2000). Remodeling dendritic spines of dentate granule cells in temporal lobe epilepsy patients and the rat pilocarpine model. Epilepsia 41 (Suppl. 6), S14–S17.

Jones, E.G., and Powell, T.P. (1969). Morphological variations in the dendritic spines of the neocortex. J. Cell Sci. 5, 509–529.

Kirov, S.A., Petrak, L.J., Fiala, J.C., and Harris, K.M. (2004). Dendritic spines disappear with chilling but proliferate excessively upon rewarming of mature hippocampus. Neuroscience 127, 69–80.

Kurz, J.E., Moore, B.J., Henderson, S.C., Campbell, J.N., and Churn, S.B. (2008). A cellular mechanism for dendritic spine loss in the pilocarpine model of status epilepticus. Epilepsia 49, 1696–1710.

Lenzlinger, P.M., Morganti-Kossmann, M.C., Laurer, H.L., and McIntosh, T.K. (2001). The duality of the inflammatory response to traumatic brain injury. Mol. Neurobiol. 24, 169–181.

Lyeth, B.G., Jenkins, L.W., Hamm, R.J., Dixon, C.E., Phillips, L.L., Clifton, G.L., Young, H.F., and Hayes, R.L. (1990). Prolonged memory impairment in the absence of hippocampal cell death following traumatic brain injury in the rat. Brain Res. 526, 249–258.

McKinney, R.A., Capogna, M., Durr, R., Gahwiler, B.H., and Thompson, S.M. (1999). Miniature synaptic events maintain dendritic spines via AMPA receptor activation. Nat. Neurosci. 2, 44–49.

Megias, M., Emri, Z., Freund, T.F., and Gulyas, A.I. (2001). Total number and distribution of inhibitory and excitatory synapses on hippocampal CA1 pyramidal cells. Neuroscience 102, 527–540.

Monfils, M.H., and Teskey, G.C. (2004). Induction of long-term depression is associated with decreased dendritic length and spine density in layers III and V of sensorimotor neocortex. Synapse 53, 114–121.

Nimchinsky, E.A., Sabatini, B.L., and Svoboda, K. (2002). Structure and function of dendritic spines. Annu. Rev. Physiol. 64, 313–353.

Niwa, R., Nagata-Ohashi, K., Takeichi, M., Mizuno, K., and Uemura, T. (2002). Control of actin reorganization by Slingshot, a family of phosphatases that dephosphorylate ADF/cofilin. Cell 108, 233–246.

Norris, C.M., and Scheff, S. (2009). Recovery of afferent function and synaptic strength in hippocampal CA1 following traumatic brain injury. J. Neurotrauma 26, 2269–2278.

Pak, D.T., and Sheng, M. (2003). Targeted protein degradation and synapse remodeling by an inducible protein kinase. Science 302, 1368–1373.

Park, J.S., Bateman, M.C., and Goldberg, M.P. (1996). Rapid alterations in dendrite morphology during sublethal hypoxia or glutamate receptor activation. Neurobiol. Dis. 3, 215–227.

Parnavelas, J.G., Lynch, G., Brecha, N., Cotman, C.W., and Globus, A. (1974). Spine loss and regrowth in hippocampus following deafferentation. Nature 248, 71–73.

Paxinos, G., and Watson, C. (1998). *The Rat Brain in Stereotaxic Coordinates*, 4th ed. Academic Press: San Diego.

Petrak, L.J., Harris, K.M., and Kirov, S.A. (2005). Synaptogenesis on mature hippocampal dendrites occurs via filopodia and immature spines during blocked synaptic transmission. J. Comp. Neurol. 484, 183–190.

Pitkanen, A., and McIntosh, T.K. (2006). Animal models of post-traumatic epilepsy. J. Neurotrauma 23, 241–261.

Ruan, Y.W., Lei, Z., Fan, Y., Zou, B., and Xu, Z.C. (2009). Diversity and fluctuation of spine morphology in CA1 pyramidal neurons after transient global ischemia. J. Neurosci. Res. 87, 61–68.

Sarmiere, P.D., and Bamburg, J.R. (2004). Regulation of the neuronal actin cytoskeleton by ADF/cofilin. J. Neurobiol. 58, 103–117.

Scheff, S.W., Price, D.A., Hicks, R.R., Baldwin, S.A., Robinson, S., and Brackney, C. (2005). Synaptogenesis in the hippocampal CA1 field following traumatic brain injury. J. Neurotrauma 22, 719–732.

Schwarzbach, E., Bonislawski, D.P., Xiong, G., and Cohen, A.S. (2006). Mechanisms underlying the inability to induce area CA1 LTP in the mouse after traumatic brain injury. Hippocampus 16, 541–550.

Schwartz, N., Schohl, A., and Ruthazer, E.S. (2009). Neural activity regulates synaptic properties and dendritic structure in vivo through calcineurin/NFAT signaling. Neuron 62, 655–669.

Seeburg, D.P., and Sheng, M. (2008). Activity-induced Polo-like kinase 2 is required for homeostatic plasticity of hippocampal neurons during epileptiform activity. J. Neurosci. 28, 6583–6591.

Seeburg, D.P., Feliu-Mojer, M., Gaiottino, J., Pak, D.T., and Sheng, M. (2008). Critical role of CDK5 and Polo-like kinase 2 in homeostatic synaptic plasticity during elevated activity. Neuron 58, 571–583.

Shankar, G.M., Bloodgood, B.L., Townsend, M., Walsh, D.M., Selkoe, D.J., and Sabatini, B.L. (2007). Natural oligomers of the Alzheimer amyloid-beta protein induce reversible synapse loss by modulating an NMDA-type glutamate receptor-dependent signaling pathway. J. Neurosci. 27, 2866–2875.

Shao, L.R., and Dudek, F.E. (2005). Electrophysiological evidence using focal flash photolysis of caged glutamate that CA1 pyramidal cells receive excitatory synaptic input from the subiculum. J. Neurophysiol. 93, 3007–3011.

Spires-Jones, T.L., Kay, K., Matsouka, R., Rozkalne, A., Betensky, R.A., and Hyman, B.T. (2011). Calcineurin inhibition with systemic FK506 treatment increases dendritic branching and dendritic spine density in healthy adult mouse brain. Neurosci. Lett. 487, 260–263.

Spruston, N., and McBain, C. (2007). Structural and functional properties of hippocampal neurons, in: *The Hippocampus Book*. P. Andersen (ed). Oxford University Press: New York, pps. 133–202.

Thompson, H.J., Lifshitz, J., Marklund, N., Grady, M.S., Graham, D.I., Hovda, D.A., and McIntosh, T.K. (2005). Lateral fluid percussion brain injury: a 15-year review and evaluation. J. Neurotrauma 22, 42–75.

Wang, Y., Shibasaki, F., and Mizuno, K. (2005). Calcium signal-induced cofilin dephosphorylation is mediated by Slingshot via calcineurin. J. Biol. Chem. 280, 12683–12689.

Wu, G.Y., Zou, D.J., Rajan, I., and Cline, H. (1999). Dendritic dynamics in vivo change during neuronal maturation. J. Neurosci. 19, 4472–4483.

Wu, L.X., Sun, C.K., Zhang, Y.M., Fan, M., Xu, J., Ma, H., and Zhang, J. (2007). Involvement of the Snk-SPAR pathway in glutamate-induced excitotoxicity in cultured hippocampal neurons. Brain Res. 1168, 38–45.

Xu, H.T., Pan, F., Yang, G., and Gan, W.B. (2007). Choice of cranial window type for in vivo imaging affects dendritic spine turnover in the cortex. Nat. Neurosci. 10, 549–551.

Zeng, L.H., Xu, L., Rensing, N.R., Sinatra, P.M., Rothman, S.M., and Wong, M. (2007). Kainate seizures cause acute dendritic injury and actin depolymerization in vivo. J. Neurosci. 27, 11604–11613.

Zhou, Q., Homma, K.J., and Poo, M.M. (2004). Shrinkage of dendritic spines associated with long-term depression of hippocampal synapses. Neuron 44, 749–757.

Zipfel, G.J., Babcock, D.J., Lee, J.M., and Choi, D.W. (2000). Neuronal apoptosis after CNS injury: the roles of glutamate and calcium. J. Neurotrauma 17, 857–869.

Address correspondence to:
Severn B. Churn, Ph.D.
Departments of Anatomy and Neurobiology
P.O. Box 980599
Virginia Commonwealth University
Richmond, VA 23298

E-mail: schurn@vcu.edu

This article has been cited by:

1. Xuewei Xia, Yuwei Dong, Yiqing Du, Yongdong Yang, Wenbo Wang, Yong Li. 2011. Relationship Between Learning and Memory Deficits and Arp2 Expression in the Hippocampus in Rats with Traumatic Brain Injury. *World Neurosurgery* . [CrossRef]